

First series of mixed (P^{III}, Se^{IV})-heteroatoms oriented rare-earth embedded polyoxotungstates containing distinct building blocks

Lulu Liu,^a Jun Jiang,^a Xiaoyi Liu,^a Guoping Liu,^a Dan Wang,^a Lijuan Chen,^{*,a} and Junwei Zhao^{*,a}

^aHenan Key Laboratory of Polyoxometalate Chemistry, College of Chemistry and Chemical Engineering, Henan University, Kaifeng, Henan 475004, China

Electronic Supplementary Information

Materials and Methods

X-ray crystallography

Fig. S1 Schematic diagram of the synthesis process of **1–8**.

Fig. S2 Comparisons of powder X-ray diffraction patterns of **1** (a), **2** (b), **3** (c), **4** (d), **5** (e), **6** (f), **7** (g), and **8** (h) with their corresponding simulated X-ray diffraction patterns from single-crystal structural analyses.

Fig. S3 IR spectra of **1–8**.

Fig. S4 (a) The 3D packing diagram of **1** viewed along the *c* axis. (b) Simplified 3D packing for **1** in *c* axis.

Fig. S5 (a) The 3D packing diagram of **1** viewed along the *a* axis. (b) Simplified 3D packing for **1** in *a* axis.

Fig. S6 The UV spectra evolutions of **1** in the acidic and alkaline direction.

Fig. S7 Comparison of CVs of bare GCE, CMWCNT-GCE and **1**@CMWCNT-GCE in 0.10 mol/L PBS (pH = 7.00) in the absence of DA and UA (scan rate: 100 mV/s).

Fig. S8 The linear relationship between peak current of DA and scan rate.

Fig. S9 The linear relationship between peak current of UA and scan rate.

Fig. S10 (a) EDS of the surface of the CMWCNT-GCE. (b) EDS of the surface of **1**@CMWCNT-GCE.

Fig. S11 TG curves of **1–8**.

Table S1. Crystallographic data and structure refinements for **1–8**.

Table S2. BVS calculations of all the oxygen atoms on Ce1³⁺ ion in **1**.^[5]

Table S3. BVS calculations of all the oxygen atoms on Ce2³⁺ ion in **1**.^[5]

Materials and methods.

All chemicals were commercially purchased and used without further purification. Elemental analyses (carbon, hydrogen and nitrogen) were performed on a Vario EL Cube CHNS analyzer. Inductively coupled plasma atomic emission spectrometry (ICP-AES) was carried out on a Perkin-Elmer Optima 2000 ICP-AES spectrometer. IR spectra were received from a solid sample palletized with KBr on a Nicolet 170 SXFT-IR spectrometer in the range of 400–4000 cm^{-1} . PXRD measurements were taken by a Bruker D8 ADVANCE apparatus with Cu $K\alpha$ radiation ($\lambda = 1.54056 \text{ \AA}$) at 293 K. TG analyses were performed under a N_2 atmosphere on a Mettler-Toledo TGA/SDTA 851^e instrument with a heating rate of 10 $^\circ\text{C}/\text{min}$ from 25 to 800 $^\circ\text{C}$. Electrochemistry measurements were performed on a Shanghai Chenhua CHI600E electrochemical workstation at room temperature based on a three electrode system, where glassy carbon electrode (GCE) acted as the working electrode, platinum gauze was used as a counter electrode and a $\text{Hg}/\text{Hg}_2\text{Cl}_2$ electrode was referenced.

Preparation of $[\text{NH}_2(\text{CH}_3)_2]_{12}\text{Na}_2[\text{Ce}_2(\text{H}_2\text{O})_7(\text{W}_4\text{O}_9)(\text{HPSeW}_{15}\text{O}_{54})(\text{SeW}_9\text{O}_{33})_2]\cdot 44\text{H}_2\text{O}$ (1). $\text{Na}_2\text{WO}_4\cdot 2\text{H}_2\text{O}$ (5.001 g, 15.161 mmol), $\text{DMA}\cdot\text{HCl}$ (2.002 g, 24.552 mmol), Na_2SeO_3 (0.251 g, 1.451 mmol) and H_3PO_3 (0.041 g, 0.500 mmol) were dissolved in 20 mL of distilled water under stirring and the pH value was adjusted to 3.20 by 6.00 mol/L HCl. The solution was heated to 40 $^\circ\text{C}$ for 20 min. Then, $\text{Ce}(\text{NO}_3)_3\cdot 6\text{H}_2\text{O}$ (0.701 g, 1.614 mmol) was added to the solution and the final pH of the solution was kept at 3.20 by 2.00 mol/L NaOH. This solution was stirred for 30 min, heated at 90 $^\circ\text{C}$ for 1 h, cooled to room temperature and filtered. Yellow block crystals of **1** were obtained for several days. Yield: *ca.* 18.03% based on $\text{Ce}(\text{NO}_3)_3\cdot 6\text{H}_2\text{O}$. Elemental analysis (%) calcd: C, 2.64; H, 1.83; N, 1.54; Se, 2.17; P, 0.28; Ce, 2.56; W, 62.22; Na, 0.42. Found (%): C, 2.55; H, 2.10; N, 1.45; Se, 2.10; P, 0.20; Ce, 2.78; W, 61.95; Na, 0.59.

Preparation of $[\text{NH}_2(\text{CH}_3)_2]_{12}\text{Na}_2[\text{Pr}_2(\text{H}_2\text{O})_7(\text{W}_4\text{O}_9)(\text{HPSeW}_{15}\text{O}_{54})(\text{SeW}_9\text{O}_{33})_2]\cdot 44\text{H}_2\text{O}$ (2). The synthetic procedure of **2** was similar to **1** except that $\text{Ce}(\text{NO}_3)_3\cdot 6\text{H}_2\text{O}$ was replaced by $\text{Pr}(\text{NO}_3)_3\cdot 6\text{H}_2\text{O}$ (0.702 g, 1.614 mmol). Green block crystals of **2** were obtained. Yield: *ca.* 16.03% based on $\text{Pr}(\text{NO}_3)_3\cdot 6\text{H}_2\text{O}$. Elemental analysis (%) calcd: C, 2.64; H, 1.84; N, 1.54; Se, 2.17; P, 0.28; Pr, 2.58; W, 62.21; Na, 0.42. Found (%): C, 2.49; H, 2.06; N, 1.48; Se, 2.04; P, 0.34; Pr, 2.80; W, 62.04; Na, 0.65.

Preparation of $[\text{NH}_2(\text{CH}_3)_2]_{12}\text{Na}_2[\text{Nd}_2(\text{H}_2\text{O})_7(\text{W}_4\text{O}_9)(\text{HPSeW}_{15}\text{O}_{54})(\text{SeW}_9\text{O}_{33})_2]\cdot 44\text{H}_2\text{O}$ (3). The synthetic procedure of **3** was similar to **1** except that $\text{Ce}(\text{NO}_3)_3\cdot 6\text{H}_2\text{O}$ was replaced by $\text{Nd}(\text{NO}_3)_3\cdot 6\text{H}_2\text{O}$ (0.699 g, 1.595 mmol). Purple block crystals of **3** were obtained. Yield: *ca.* 17.23% based on $\text{Nd}(\text{NO}_3)_3\cdot 6\text{H}_2\text{O}$ based on $\text{Nd}(\text{NO}_3)_3\cdot 6\text{H}_2\text{O}$. Elemental analysis (%) calcd: C, 2.63; H, 1.83; N, 1.54; Se, 2.17; P, 0.28; Nd, 2.64; W, 62.17; Na, 0.42. Found (%): C, 2.46; H, 2.25; N, 1.50; Se, 2.06; P, 0.23; Nd, 2.73; W, 61.70; Na, 0.51.

Preparation of $[\text{NH}_2(\text{CH}_3)_2]_{12}\text{Na}_2[\text{Sm}_2(\text{H}_2\text{O})_7(\text{W}_4\text{O}_9)(\text{HPSeW}_{15}\text{O}_{54})(\text{SeW}_9\text{O}_{33})_2]\cdot 44\text{H}_2\text{O}$ (4). The synthetic procedure of **4** was similar to **1** except that $\text{Ce}(\text{NO}_3)_3\cdot 6\text{H}_2\text{O}$ was replaced by $\text{Sm}(\text{NO}_3)_3\cdot 6\text{H}_2\text{O}$ (0.701 g, 1.577 mmol). Pale yellow block crystals of **4** were obtained. Yield: *ca.* 15.83% based on $\text{Sm}(\text{NO}_3)_3\cdot 6\text{H}_2\text{O}$. Elemental analysis (%) calcd: C, 2.63; H, 1.83; N, 1.53; Se, 2.16; P, 0.28; Sm, 2.75; W, 62.10; Na, 0.42. Found (%): C, 2.41; H, 2.18; N, 1.46; Se, 2.02; P, 0.19; Sm, 2.88; W, 62.33; Na, 0.56.

Preparation of $[\text{NH}_2(\text{CH}_3)_2]_{12}\text{Na}_2[\text{Gd}_2(\text{H}_2\text{O})_7(\text{W}_4\text{O}_9)(\text{HPSeW}_{15}\text{O}_{54})(\text{SeW}_9\text{O}_{33})_2]\cdot 44\text{H}_2\text{O}$ (5). The synthetic procedure of **5** was similar to **1** except that $\text{Ce}(\text{NO}_3)_3\cdot 6\text{H}_2\text{O}$ was replaced by $\text{Gd}(\text{NO}_3)_3\cdot 6\text{H}_2\text{O}$ (0.705 g, 1.562 mmol). White block crystals of **5** were obtained. Yield: *ca.* 19.04%

based on $\text{Gd}(\text{NO}_3)_3 \cdot 6\text{H}_2\text{O}$. Elemental analysis (%) calcd: C, 2.63; H, 1.83; N, 1.53; Se, 2.16; P, 0.28; Gd, 2.87; W, 62.02; Na, 0.42. Found (%): C, 2.48; H, 2.14; N, 1.39; Se, 2.02; P, 0.21; Gd, 3.00; W, 61.87; Na, 0.51.

Preparation of $[\text{NH}_2(\text{CH}_3)_2]_{12}\text{Na}_2[\text{Tb}_2(\text{H}_2\text{O})_7(\text{W}_4\text{O}_9)(\text{HPSeW}_{15}\text{O}_{54})(\text{SeW}_9\text{O}_{33})_2] \cdot 44\text{H}_2\text{O}$ (6). The synthetic procedure of **6** was similar to **1** except that $\text{Ce}(\text{NO}_3)_3 \cdot 6\text{H}_2\text{O}$ was replaced by $\text{Tb}(\text{NO}_3)_3 \cdot 6\text{H}_2\text{O}$ (0.702 g, 1.550 mmol). Colorless block crystals of **6** were obtained. Yield: *ca.* 19.64% based on $\text{Tb}(\text{NO}_3)_3 \cdot 6\text{H}_2\text{O}$. Elemental analysis (%) calcd: C, 2.63; H, 1.83; N, 1.53; Se, 2.16; P, 0.28; Tb, 2.90; W, 62.00; Na, 0.42. Found (%): C, 2.53; H, 1.99; N, 1.37; Se, 2.10; P, 0.37; Tb, 3.11; W, 61.79; Na, 0.53.

Preparation of $[\text{NH}_2(\text{CH}_3)_2]_{12}\text{Na}_2[\text{Ho}_2(\text{H}_2\text{O})_7(\text{W}_4\text{O}_9)(\text{HPSeW}_{15}\text{O}_{54})(\text{SeW}_9\text{O}_{33})_2] \cdot 44\text{H}_2\text{O}$ (7). The synthetic procedure of **7** was similar to **1** except that $\text{Ce}(\text{NO}_3)_3 \cdot 6\text{H}_2\text{O}$ was replaced by $\text{Ho}(\text{NO}_3)_3 \cdot 6\text{H}_2\text{O}$ (0.701 g, 1.527 mmol). Light yellow block crystals of **7** were obtained. Yield: *ca.* 20.65% based on $\text{Ho}(\text{NO}_3)_3 \cdot 6\text{H}_2\text{O}$. Elemental analysis (%) calcd: C, 2.62; H, 1.83; N, 1.53; Se, 2.16; P, 0.28; Ho, 3.00; W, 61.94; Na, 0.42. Found (%): C, 2.49; H, 1.89; N, 1.43; Se, 2.07; P, 0.26; Ho, 3.15; W, 62.79; Na, 0.59.

Preparation of $[\text{NH}_2(\text{CH}_3)_2]_{12}\text{Na}_2[\text{Er}_2(\text{H}_2\text{O})_7(\text{W}_4\text{O}_9)(\text{HPSeW}_{15}\text{O}_{54})(\text{SeW}_9\text{O}_{33})_2] \cdot 44\text{H}_2\text{O}$ (8). The synthetic procedure of **8** was similar to **1** except that $\text{Ce}(\text{NO}_3)_3 \cdot 6\text{H}_2\text{O}$ was replaced by $\text{Er}(\text{NO}_3)_3 \cdot 6\text{H}_2\text{O}$ (0.702 g, 1.522 mmol). Pink block crystals of **8** were obtained. Yield: *ca.* 21.03% based on $\text{Er}(\text{NO}_3)_3 \cdot 6\text{H}_2\text{O}$. Elemental analysis (%) calcd: C, 2.62; H, 1.83; N, 1.53; Se, 2.16; P, 0.28; Er, 3.04; W, 61.91; Na, 0.42. Found (%): C, 2.43; H, 1.87; N, 1.41; Se, 2.13; P, 0.31; Er, 3.01; W, 61.39; Na, 0.47.

Preparation of **1@CMWCNT-modified GCE (named as **1**@CMWCNT-GCE):** (a) **1**@CMWCNT-GCE was prepared as follows: **1** (30.00 mg) and 10.00 mg CMWCNT were dispersed in high purity water (1 mL) under ultrasonication for 6 h to obtain a homogeneous suspension. (b) The suspension was centrifuged for 20 min at a rate of 12,000 r/min. Then the supernatant was poured out, the high purity water (1 mL) was added and the precipitate was treated by ultrasonic cleaning for 20 min at a rate of 12,000 r/min. The precipitate was washed two times in the same method. (c) The precipitate was dried at 60 °C for 3 days. The 1.00 mg precipitate together with 0.01 mL nafion was dispersed in 0.99 mL ultrapure water under ultrasonic for 30 min to form a suspension again. Before modification, the surface of GCE was polished to smoothness with 0.50 and 0.05 μm alumina slurry, and washed with ethanol and water. (d) The 10 μL suspension was dropped on the surface of cleaned GCE and dried in the air, forming the **1**@CMWCNT-GCE ECS. In addition, chemical components on the surface of the **1**@CMWCNT-GCE ECS have been confirmed by using the energy dispersive spectrometry (EDS) (Figure S10) and the results indicate that **1** and CMWCNT have been loaded onto the surface of GCE because of the existence of the signals of C, W, Pr, Se and P elements. (e) The **1**@CMWCNT-GCE ECS should be activated in 0.10 mol/L PBS in the potential range of -1.00 – 1.00 V at a scan rate of 100 mV/s for 30 cycles and then washed with water before using.

Experimental methods. 0.10 mol/L PBS solution was obtained by dissolving 6.90 g $\text{NaH}_2\text{PO}_4 \cdot 2\text{H}_2\text{O}$ and 17.91 g $\text{Na}_2\text{HPO}_4 \cdot 12\text{H}_2\text{O}$ in the 1000 mL ultrapure water. DA and UA were dissolved in 0.10 mol/L PBS to prepare different concentration solutions. CV response curves of **1**@CMWCNT-GCE were measured in 50 mL 0.10 mol/L PBS (pH = 7.00) containing DA or UA ($c(\text{DA}/\text{UA}) = 1.00$ mmol/L) in the voltage range of -1.00 – 1.00 V at a sweep rate of 100 mV/s (Figure 7a). Provided that other conditions are invariant, comparison of CVs of bare GCE, CMWCNT-GCE and

1@CMWCNT-GCE in 1.00 mmol/L DA, UA, DA and UA (Figure 7b-d). Then, the CV response of **1**@CMWCNT-GCE to DA and UA was verified for 180 cycles (cycle: 1, 10, 20, 30, 40, 60, 80, 100, 120, 140, 160, 180, Figure 8e). Next, CV curves of **1**@CMWCNT-GCE to DA and UA were discussed when scanning rate (v) varies from 20 to 200 mV/s. ($v = 20, 40, 60, 80, 100, 120, 140, 160, 180,$ and 200 mV/s, Figure 7f). In the end, the changes in peak current of DA or/and UA were determined using **1**@CMWCNT-GCE ECS to serve as a working electrode with DA or/and UA concentration changing from 10–100 or 2–200 $\mu\text{mol/L}$ (Figure 8a-c).

X-ray crystallography.

Single-crystal X-ray diffraction data of **1–8** were collected on a Bruker APEX-II CCD detector at 150 K with Mo $K\alpha$ radiation ($\lambda = 0.71073 \text{ \AA}$). Direct methods were used to solve their structures and locate the heavy atoms using the SHELXTL-97 program package.¹ The remaining atoms were found from successive full-matrix least-squares refinements on F^2 and Fourier syntheses. Lorentz polarization and SADABS corrections were applied. All hydrogen atoms attached to carbon and nitrogen atoms were geometrically placed and refined isotropically as a riding model using the default SHELXTL parameters. No hydrogen atoms associated with water molecules were located from the difference Fourier map. All non-hydrogen atoms except for some Na, C, N, O and some water atoms were refined anisotropically. However, there are still solvent accessible voids accessible solvent voids in the check cif reports of crystal structures, suggesting that some lattice water molecules and counter cations should exist in the structures, which can't be found from the weak residual electron peaks. These lattice water molecules and counter cations are highly disordered and attempts to locate and refine them were unsuccessful. On the basis of elemental analysis and TG analysis, twenty-four lattice water molecules and four $[\text{H}_2\text{N}(\text{CH}_3)_2]^+$ cations for **1**, thirty-six lattice water molecules, one Na^+ cation and four $[\text{H}_2\text{N}(\text{CH}_3)_2]^+$ cations for **2-4**, twenty-seven lattice water molecules and four $[\text{H}_2\text{N}(\text{CH}_3)_2]^+$ cations for **5**, eighteen lattice water molecules and three $[\text{H}_2\text{N}(\text{CH}_3)_2]^+$ cations for **6**, thirty-six lattice water molecules, one Na^+ cation and four $[\text{H}_2\text{N}(\text{CH}_3)_2]^+$ cations for **7** and eighteen lattice water molecules and three $[\text{H}_2\text{N}(\text{CH}_3)_2]^+$ cations for **8** were directly added to the molecular formula. The crystallographic data and structure refinement parameters for **1–8** are demonstrated in Table S1. Crystallographic data and structure refinements for **1–8** reported in this paper have been deposited in the Cambridge Crystallographic Data Centre with CCDC 2023680–2023685 and 2033453–2033454. These data can be obtained free of charge from the Cambridge Crystallographic Data Centre via www.ccdc.cam.ac.uk/data_request/cif.

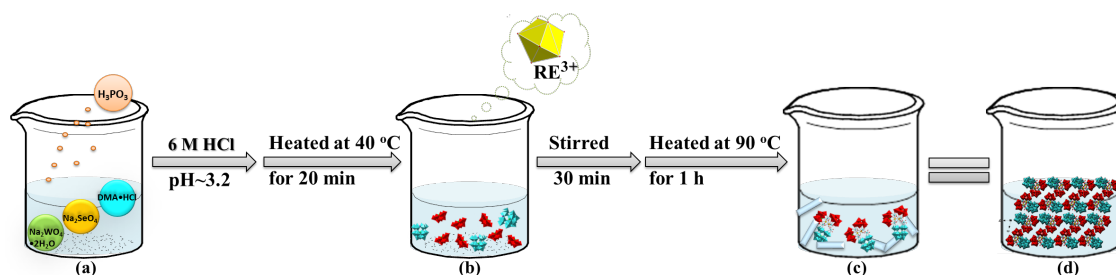


Fig. S1 Schematic diagram of the synthesis process of **1–8**.

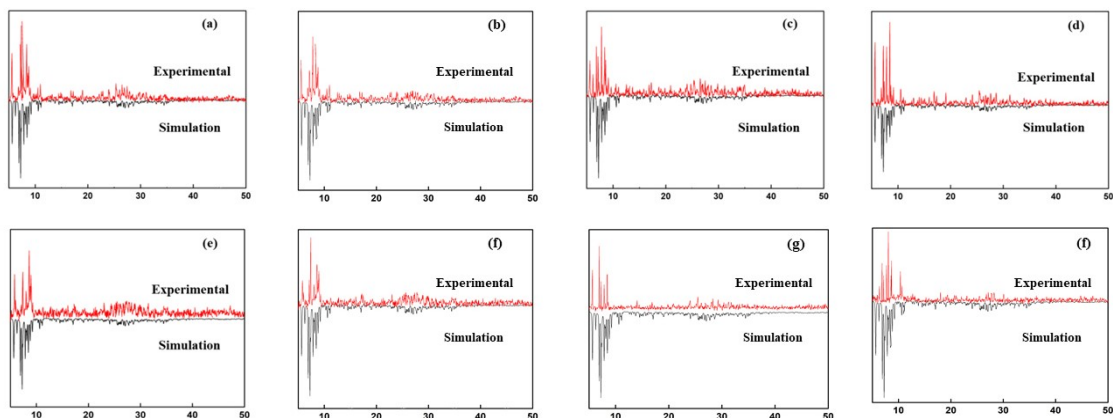


Fig. S2 Comparisons of powder X-ray diffraction patterns of **1** (a), **2** (b), **3** (c), **4** (d), **5** (e), **6** (f), **7** (g) and **8** (h) with their corresponding simulated X-ray diffraction patterns from single-crystal structural analyses.

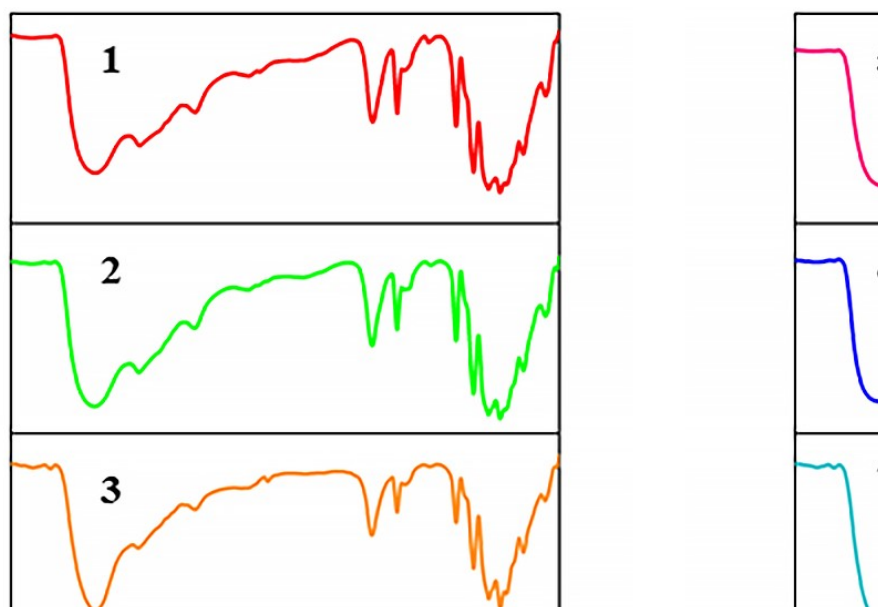


Fig. S3 IR spectra of **1–8**.

IR spectra of **1–8** are further measured between 4000 and 400 cm^{-1} on a Nicolet 170 SXFT-IR spectrometer by employing KBr pellets (Fig. S3). All the spectra have similar vibration modes, indicating that **1–8** have the same basic structural framework. Four characteristic vibration $\nu(\text{W}-\text{O}_i)$, $\nu(\text{Se}-\text{O}_a)$, $\nu(\text{W}-\text{O}_b)$, and $\nu(\text{W}-\text{O}_c)$ are observed at 962, 864, 789, 738 cm^{-1} for **1**, 962, 864, 788, 735 cm^{-1} for **2**, 962, 863, 788, 736 cm^{-1} for **3**, 962, 862, 788, 739 cm^{-1} for **4**, 962, 868, 789, 735 cm^{-1} for **5**, 962, 868, 787, 732 cm^{-1} for **6**, 962, 866, 788, 735 cm^{-1} for **7**, 962, 868, 786, 734 cm^{-1} for **8**, severally.² The characteristic peak at 1075–1080 cm^{-1} corresponds to the $\nu(\text{P}-\text{O})$ vibration. In addition, the appearance of a broad vibration band located in the range of 3434–3457 cm^{-1} is indicative of the presence of lattice or coordination water molecules in **1–8**,³ whereas two weak bands appearing at 3155–3165 cm^{-1} and 2785–2796 cm^{-1} are respectively assigned to the N–H and C–H stretching vibrations, illustrating the presence of dimethylamine components. Notably, the RE–O stretching vibrations are unseen in the IR region of **1–8**, mainly because of predominant ionic interactions between RE cations and ST fragments.⁴

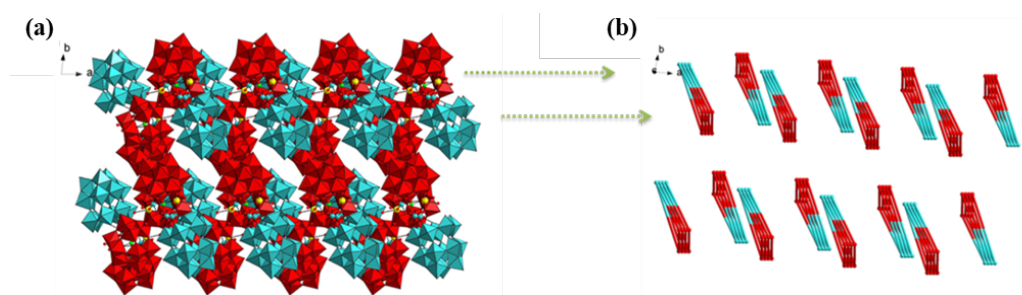


Fig. S4 (a) The 3D packing diagram of **1** viewed along the *c* axis. (b) Simplified 3D packing for **1** in *c* axis.

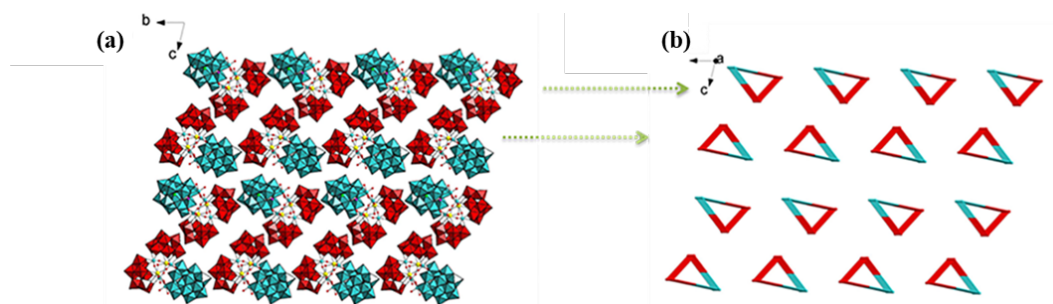


Fig. S5 (a) The 3D packing diagram of **1** viewed along the *a* axis. (b) Simplified 3D packing for **1** in *a* axis.

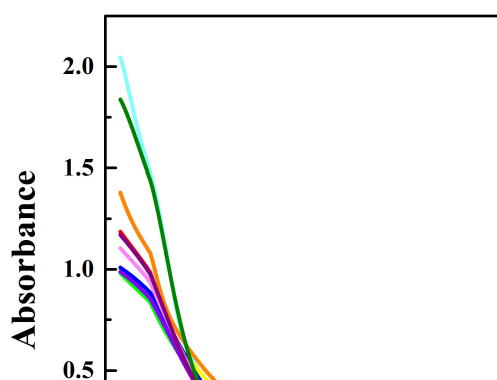


Fig. S6 The UV spectra evolution of **1** in the acidic and alkaline direction.

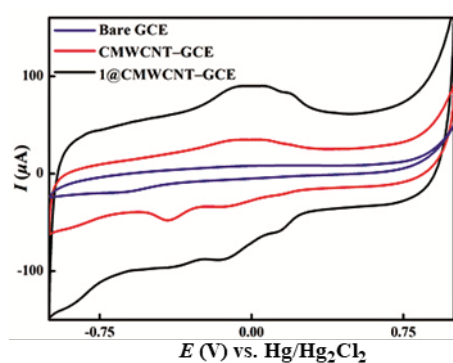


Fig. S7 Comparison of CVs of bare GCE, CMWCNT-GCE and **1**@CMWCNT-GCE in 0.10 mol/L PBS (pH = 7.00) in the absence of DA and UA (scan rate: 100 mV/s).

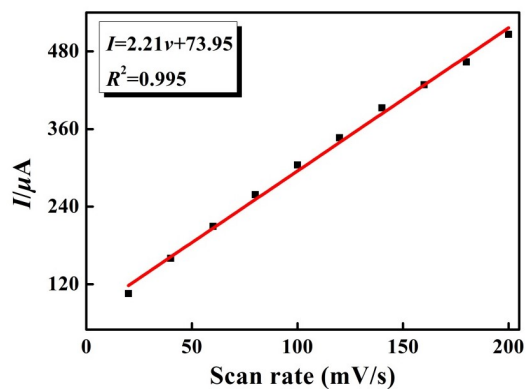


Fig. S8 The linear relationship between peak current of DA and scan rate.

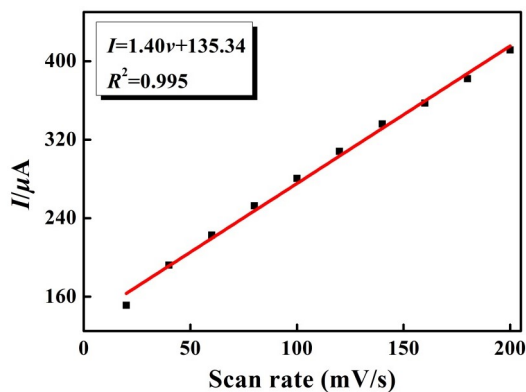


Fig. S9 The linear relationship between peak current of UA and scan rate.

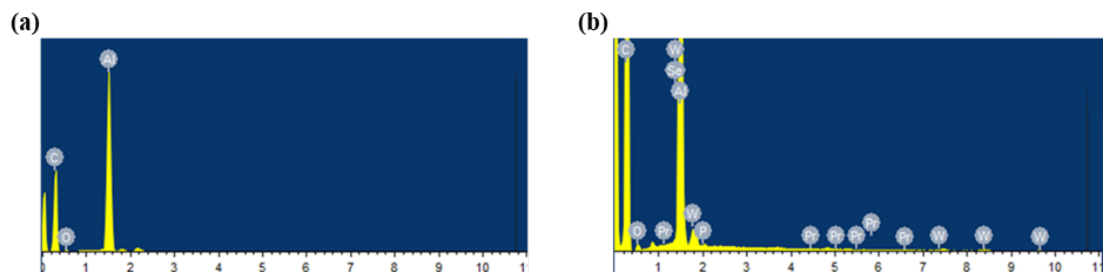


Fig. S10 (a) EDS of the surface of the CMWCNT-GCE. (b) EDS of the surface of **1**@CMWCNT-GCE.

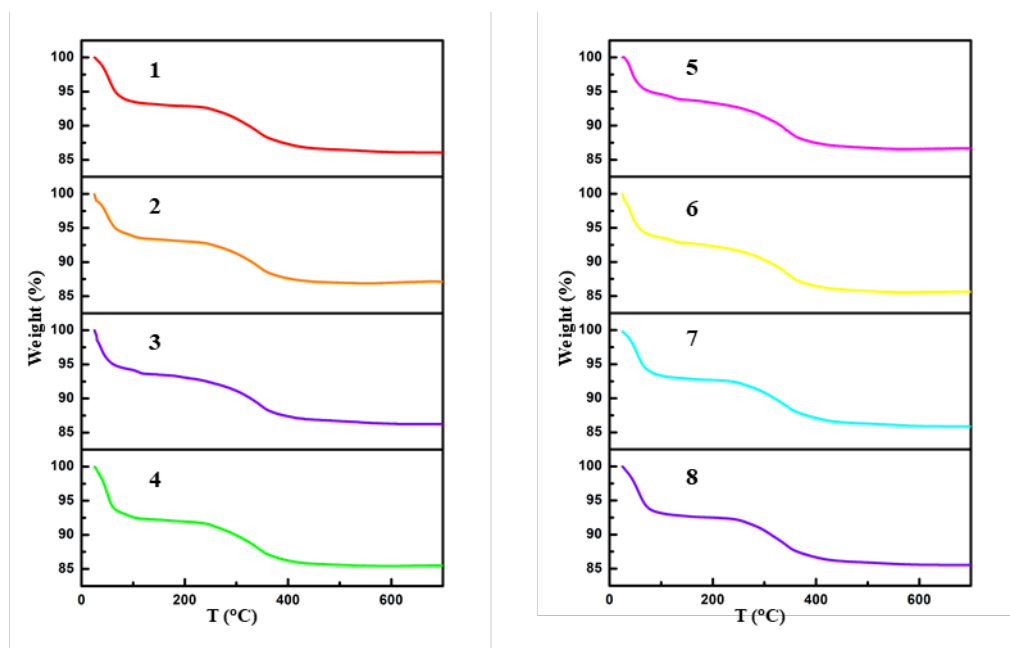


Fig. S11 TG curves of **1–8**.

The thermogravimetric measurements of **1–8** were performed under the flowing N_2 atmosphere from 25 to 700 °C on solid crystalline samples. As exhibited in Figure S11, these compounds display almost analogous two-step slow weight loss process. From 25 to 180 °C, the weight loss 6.96% (calcd. 7.24%) for **1**, 6.85% (calcd. 7.24%) for **2**, 7.44% (calcd. 7.24%) for **3**, 7.12% (calcd. 7.23%) for **4**, 7.46% (calcd. 7.22%) for **5**, 7.66% (calcd. 7.22 %) for **6**, 7.32% (calcd. 7.21%) for **7**, 7.46% (calcd. 7.21 %) for **8** is attributed to the liberation of 44 lattice water molecules. Upon heating to 700 °C, the second weight loss of 14.72% (calcd. 15.08%) for **1**, 14.72% (calcd. 15.08%) for **2**, 14.46% (calcd. 15.07 %) for **3** and 15.07% (calcd. 15.05 %) for **4**, 14.11% (calcd. 15.04%) for **5**, 14.75% (calcd. 15.03%) for **6**, 14.55% (calcd. 15.01%) for **7**, 14.68% (calcd. 15.01%) for **8** is attributed to seven coordination water molecules, dimethylamine groups as well as the dehydration of twelve protons and the sublimation of 0.50 P_2O_5 . Overall, the weight loss courses of all members mentioned in this paper agree with the theoretical outcomes well as expected.

Table S1. Crystallographic data and structure refinements for 1–8.

	1	2	3	4
CCDC	2023680	2023681	2023682	2023683
Empirical formula	$C_{24}H_{199}N_{12}O_{180}Na_2$ $PSe_3Ce_2W_{37}$	$C_{24}H_{199}N_{12}O_{180}Na_2$ $PSe_3Pr_2W_{37}$	$C_{24}H_{199}N_{12}O_{180}Na_2$ $PSe_3Nd_2W_{37}$	$C_{24}H_{199}N_{12}O_{180}Na_2$ $PSe_3Sm_2W_{37}$
Formula weight	10933.47	10935.05	10941.71	10953.93
Crystal system	Triclinic	Triclinic	Triclinic	Triclinic
Space group	<i>P</i> -1	<i>P</i> -1	<i>P</i> -1	<i>P</i> -1
<i>a</i> , Å	14.1165(16)	14.2229(6)	14.2245(3)	14.2090(3)
<i>b</i> , Å	21.127(3)	21.3543(8)	21.3449(4)	21.3290(5)
<i>c</i> , Å	32.262(4)	32.7480(12)	32.7499(7)	32.6694(6)
α , deg	76.631(4)	76.4620(10)	76.4550(10)	76.5270(10)
β , deg	88.057(4)	88.8950(10)	88.9920(10)	89.0640(10)

γ , deg	83.473(4)	83.6120(10)	83.5640(10)	83.3840(10)
V , Å ³	9300.0(19)	9609.6(6)	9605.7(3)	9563.8(3)
Z	2	2	2	2
μ , mm ⁻¹	23.976	23.236	23.279	23.452
$F(000)$	9720	9724	9728	9736
D_c , g cm ⁻³	3.904	3.779	3.783	3.804
T , K	254(2)	296(2)	296(2)	296(2)
	$-16 \leq h \leq 16$			
Limiting indices	$-25 \leq k \leq 25$			
	$-38 \leq l \leq 38$			
Reflections collected/unique	77712 / 32307	104942 / 33677	102872 / 33697	104879 / 33539
R_{int}	0.0638	0.0352	0.0588	0.0547
Data/restraints/parameters	32307 / 162 / 1922	33677 / 3 / 1830	33697 / 5 / 1826	33539 / 14 / 1826
GOF on F^2	1.021	1.030	1.088	1.021
R_1, wR_2 ($I > 2\sigma(I)$) ^a	0.0645, 0.1620	0.0334, 0.0899	0.0457, 0.1298	0.0464, 0.1131
R_1, wR_2 (all data)	0.0920, 0.1794	0.0424, 0.0934	0.0680, 0.1388	0.0787, 0.1261
	5	6	7	8
CCDC	2023684	2023685	2033453	2033454
Empirical formula	C ₂₄ H ₁₉₉ N ₁₂ O ₁₈₀ Na ₂ PSe ₃ Gd ₂ W ₃₇	C ₂₄ H ₁₉₉ N ₁₂ O ₁₈₀ Na ₂ PSe ₃ Tb ₂ W ₃₇	C ₂₄ H ₁₉₉ N ₁₂ O ₁₈₀ Na ₂ PSe ₃ Ho ₂ W ₃₇	C ₂₄ H ₁₉₉ N ₁₂ O ₁₈₀ Na ₂ PSe ₃ Er ₂ W ₃₇
Formula weight	10967.73	10971.07	11006.08	11010.7
Crystal system	Triclinic	Triclinic	Triclinic	Triclinic
Space group	<i>P</i> -1	<i>P</i> -1	<i>P</i> -1	<i>P</i> -1
a , Å	14.1026(8)	14.1563(6)	14.234(3)	14.1132(4)
b , Å	21.1950(11)	21.2367(9)	21.282(5)	21.1838(6)
c , Å	31.9639(18)	32.4204(16)	32.772(8)	32.3595(8)
α , deg	76.572(2)	77.002(2)	76.696(9)	76.9730(10)
β , deg	88.809(2)	89.953(2)	89.375(8)	89.9770(10)
γ , deg	83.008(2)	83.060(2)	83.283(9)	82.8850(10)
V , Å ³	9223.6(9)	9423.8(7)	9594(4)	9349.2(4)
Z	2	2	2	2
μ , mm ⁻¹	24.400	23.928	23.594	24.262
$F(000)$	9744	9748	9778	9782
D_c , g cm ⁻³	3.949	3.866	3.810	3.911
T , K	150(2)	150(2)	300(2) K	150(2) K
	$-16 \leq h \leq 16$			
Limiting indices	$-25 \leq k \leq 25$			
	$-38 \leq l \leq 38$			
Reflections	84810 / 32241	100889 / 33017	75838 / 32469	86878 / 32744

collected/unique				
R_{int}	0.0693	0.0831	0.0421	0.0330
Data/restraints/parameters	32241 / 42 / 1884	33017 / 60 / 1920	32469 / 5 / 1815	32744 / 21 / 1961
GOF on F^2	1.039	1.007	1.075	1.040
R_1, wR_2 ($I > 2\sigma(I)$) ^a	0.0632, 0.1465	0.0496, 0.1125	0.0451, 0.1279	0.0368, 0.0852
R_1, wR_2 (all data)	0.0985, 0.1599	0.0785, 0.1239	0.0667, 0.1374	0.0430, 0.0876

Table S2. BVS calculations of all the oxygen atoms on Ce1³⁺ ion in 1.^[5]

Atom	O19	O47	O71	O118	O119	O1W	O2W	O3W
BVS	1.90	2.18	1.84	1.98	1.99	0.29	0.38	0.31

Table S3. BVS calculations of all the oxygen atoms on Ce2³⁺ ion in 1.^[5]

Atom	O2	O46	O74	O76	O78	O114	O4W	O5W
BVS	1.96	2.00	2.03	2.01	1.96	2.03	0.32	0.40

References

- [1] (a) G. M. Sheldrick, SADABS: Program for Absorption Correction, University of Göttingen: Göttingen, Germany, 1997; (b) G. M. Sheldrick, SHELXS 97, Program for Crystal Structure Solution, University of Göttingen, Göttingen, Germany, 1997; (c) G. M. Sheldrick, SHELXL 97, Program for Crystal Structure Refinement, University of Göttingen, Germany, 1997.
- [2] (a) W. C. Chen, H. L. Li, X. L. Wang, K. Z. Shao, Z. M. Su and E. B. Wang, Assembly of cerium(III)-stabilized polyoxotungstate nanoclusters with $\text{SeO}_3^{2-}/\text{TeO}_3^{2-}$ templates: from single polyoxoanions to inorganic hollow spheres in dilute solution, *Chem. Eur. J.*, 2013, **19**, 11007–11015; (b) H. L. Li, W. Yang, Y. Chai, L. J. Chen and J. W. Zhao, A novel Dawson-like cerium(IV)-hybridizing selenotungstate $\text{Na}_{13}\text{H}_7[\text{Ce}(\text{SeW}_{17}\text{O}_{59})_2]\cdot 31\text{H}_2\text{O}$, *Inorg. Chem. Commun.*, 2015, **56**, 35–40.
- [3] (a) K. C. Szeto, K. P. Lillerud, M. Tilset, M. Bjørgen, C. Prestipino, A. Zecchina, C. Lamberti and S. Bordiga, A thermally stable Pt/Y-based metal–organic framework: exploring the accessibility of the metal centers with spectroscopic methods using H_2O , CH_3OH , and CH_3CN as probes, *J. Phys. Chem. B*, 2006, **110**, 21509–21520; (b) S. Bordiga, A. Damin, F. Bonino, A. Zecchina, G. Spanò, F. Rivetti, V. Bolis, C. Prestipino and C. Lamberti, Effect of interaction with H_2O and NH_3 on the vibrational, electronic, and energetic peculiarities of Ti(IV) centers TS-1 catalysts: a spectroscopic and computational study, *J. Phys. Chem. B*, 2002, **106**, 9892–9905.
- [4] (a) J. W. Zhao, C. M. Wang, J. Zhang, S. T. Zheng and G. Y. Yang, Combination of lacunary polyoxometalates and high-nuclear transition metal clusters under hydrothermal conditions: IX. a Series of novel polyoxotungstates sandwiched by octa-copper clusters, *Chem. Eur. J.*, 2008, **14**, 9223–9239; (b) S. W. Zhang, J. W. Zhao, P. T. Ma, J. Y. Niu and J. P. Wang, Rare-earth-transition-metal organic-inorganic hybrids based on Keggin-type polyoxometalates and pyrazine-2,3-dicarboxylate, *Chem. Asian J.*, 2012, **7**, 966–974; (c) J. W. Zhao, H. L. Li, Y. Z. Li, C. Y. Li, Z. L. Wang and L. J. Chen, Rectangle versus square oxalate-connective tetralanthanide cluster anchored in lacunary lindqvist isopolytungstates: syntheses, structures, and properties, *Cryst. Growth Des.*, 2014, **14**, 5495–5505.

[5] (a) A. Trzesowska, R. Kruszynski and T. J. Bartczak, New bond-valence parameters for lanthanides, *Acta Cryst.*, 2004, **B60**, 174–178; (b) I. D. Brown and D. Altermatt, Bond-valence parameters obtained from a systematic analysis of the inorganic crystal structure database, *Acta Cryst.*, 1985, **B41**, 244–247.